Imaging Agents

DOI: 10.1002/anie.201006195

# Coupling of Luminescent Terbium Complexes to $Fe_3O_4$ Nanoparticles for Imaging Applications**

*Baodui Wang, Jun Hai, Qin Wang, Tianrong Li, and Zhengyin Yang**

Coupling optically active components to magnetic nanoparticles (NPs) is an attractive way to develop multifunctional probes for highly sensitive biological imaging and recognition.[1] While iron oxide NPs have been explored as robust magnetic contrast and therapeutic agents,[2] semiconducting quantum dots, fluorescent organic dyes, and metal complexes are now commonly sought after for sensitive optical imaging applications.[3] Among all molecular optical probes studied thus far, lanthanide-based complexes have attracted particular interest due to their unique long luminescence lifetimes (micro- to milliseconds), sharp emission bands, and insensitivity to photobleaching.[4] Despite numerous efforts researching magnetic NPs and lanthanide-based complexes for biomedical applications, conjugates containing both magnetic NPs and lanthanide complexes have not been synthesized and studied. Such conjugates with both magnetic and optical imaging capabilities should serve as new bifunctional probes for highly sensitive biorecognition applications.

We have now designed and prepared a luminescent lanthanide nanoparticle label based on sensitization of an organic chromophore. The particle is made up of $Fe_3O_4$ NPs coated with a lanthanide complex (Scheme 1). Ligand **1b** is comprised of a quinolone-based dye acting as light-absorption antenna and a polyethylene glycol 3,4-dihydroxybenzylamine (DBI-PEG-$NH_2$) moiety, which enables binding to the surface of $Fe_3O_4$ NPs to give water-soluble NPs. These $Fe_3O_4$ NPs are strongly luminescent in aqueous solution and have a long fluorescence lifetime.

Folic acid (FA) is a high-affinity ligand for folate receptor (FR), and has been widely used for targeted delivery of FA-conjugated molecular probes or nanoparticles to FR-overexpressing cancer cell lines (e.g., HeLa and KB cell lines).[5] Since salicylic acid has excellent coordination ability with rare-earth metal ions and can sensitize their luminescence,[6] we used folate-(salicylic acidyl)-amine as cell-targeting agent for further application in bioimaging based on Tb:**1b**.

Synthesis of the luminescent $Fe_3O_4$ NPs is presented in Scheme S1 (Supporting Information). The PEG amine **1a** was prepared from 1,ω-diaminopolyoxyethylene ($M = 4000$) and 3,4-dihydroxybenzaldehyde. 7-Amino-4-methyl-2(1*H*)-quinolinone (cs124) was covalently coupled with diethylenetriaminepentaacetic acid (DTPA) by means of its dianhydride, and the product was then treated with **1a** to obtain **1b**. Complex Tb:**1b** was formed by stirring **1b** with $TbCl_3$ overnight in DMF, and then treated with folate-(salicylic acidyl)-amine in DMF to give Tb:**1b**-FA. Monodisperse $Fe_3O_4$ NPs coated with oleylamine with a size of 12 nm were synthesized by a previously published procedure.[7] Exchange of oleic acid and oleylamine on the surface of $Fe_3O_4$ NPs with Tb:**1b** or Tb:**1b**-FA was easily achieved by mixing Tb:**1b** or Tb:**1b**-FA and $Fe_3O_4$ NPs monodispersed in water (Figure S1, Supporting Information); the NPs showed little change in core size after surface modification. According to the Tb/Fe weight percentage (105%), about 2312 Tb units are bound to each $Fe_3O_4$ NP, corresponding to about 2312 ligands per $Fe_3O_4$ NP.[8] Magnetization of as-synthesized $Fe_3O_4$ NPs and Tb:**1b**-FA-NPs was measured as a function of applied magnetic field (Figure S2, Supporting Information). Little change in magnetic properties was observed between the as-synthesized $Fe_3O_4$ NPs and Tb:**1b**-FA-NPs. None of the samples showed hysteresis, that is, the nanoparticles retain superparamagetism. The saturated magnetization ($M_s$) of as-synthesized $Fe_3O_4$ NPs and Tb:**1b**-NPs are 54.8 and 17.8 $A\,m^2\,kg^{-1}$, respectively.

The dispersibility of Tb:**1b**-FA-NPs was tested by measuring the change of their hydrodynamic size during incubation under different conditions. Figure S3 (Supporting Information) shows that Tb:**1b**-FA-NPs are stable to dispersion in phosphate buffered saline (PBS) and show no change in the statistical hydrodynamic size over the incubation time, and little change in the size of Tb:**1b**-FA-NPs occurs with varying temperature. The measured size increase from about 129 to about 219 nm in the presence of fetal bovine serum (FBS) is attributed to adsorption of FBS onto the NP surface, as reported previously.[9] On the other hand, at lower pH 6 (Figure S4, Supporting Information), the particles can be stabilized for only 2 h before serious aggregation occurs. After 8 h, the size of the clustered nanoparticles reaches 190 nm, due to chemical bond cleavage between iron oxide and the catechol unit of 3,4-dihydroxybenzaldehyde under low-pH incubation conditions, which destabilizes the nanoparticle dispersion.[10]

[*] B. Wang
Key Laboratory of Nonferrous Metal Chemistry and Resources Utilization of Gansu Province and State Key Laboratory of Applied Organic Chemistry, Lanzhou University (P.R. China)
J. Hai, T. Li, Z. Yang
College of Chemistry and Chemical Engineering, Lanzhou University
Gansu, Lanzhou, 730000 (P. R. China)
Fax: (+86) 931-891-2582
E-mail: yangzy@lzu.edu.cn
Q. Wang
College of Life Science, Lanzhou University (P.R. China)

[**] The work was supported by the National Natural Science Foundation of China (20975046), the Fundamental Research Funds for the Central Universities (lzujbky-2010-35), and the Specialized Research Fund for the Doctoral Program of Higher Education (20100211120010).

Supporting information for this article is available on the WWW under http://dx.doi.org/10.1002/anie.201006195.

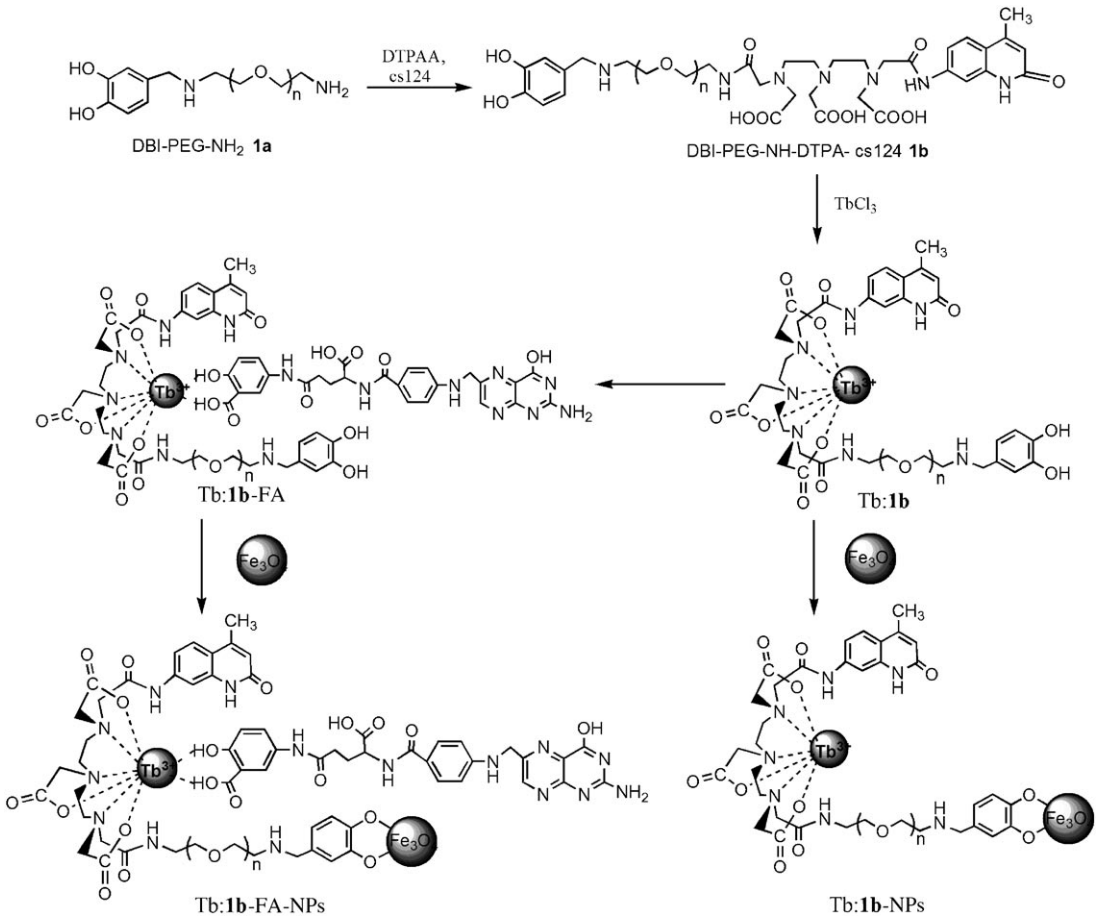


***Scheme 1.*** Structures and schematic illustrations of **1a**, **1b**, Tb:**1b**, Tb:**1b**-FA, Tb:**1b**-NPs, and Tb:**1b**-FA-NPs.

Since the crystal structure of the $Tb^{III}$ complex has not been obtained yet, we characterized the complex and determined its possible structure by mass spectrometry, fluorescence spectroscopy, and IR spectroscopy. The structure of the complex that is likely—based on the spectroscopic data and the literature[11]—is shown in Figure 1. The mass spectrum of the complex shows a peak at *m*/*z* 706 which can be assigned to the ion pair $[Tb\text{-DTPA-cs124+H}]^+$ (Figure S5, Supporting Information).

Figure S6 (Supporting Information) shows fluorescence spectra of Tb:**1b** in deionized (DI) water at an excitation wavelength of $\lambda_{max} = 325$. The linelike emission peaks of Tb:**1b** at 490, 546, 585, and 621 nm arise from transitions of Tb from its $^5D_4$ state to its $^7F_6$, $^7F_5$, $^7F_4$, and $^7F_3$ ground states, respectively.[12] The same fluorescence spectra were also obtained for Tb:**1b**-FA, Tb:**1b**-NPs, and Tb:**1b**-FA-NPs (Figures S7–S9, Supporting Information). Tb:4-amino-salicylic acid also emits the characteristic fluorescence of $Tb^{3+}$ (Figure S10, Supporting Information). Interestingly, the emission intensity of Tb:**1b** increases with increasing concentration of folate-(salicylic acidyl)-amine (Figure S11, Supporting Information).

The structures of Tb:**1b**, Tb:**1b**-FA, Tb:**1b**-NPs, and Tb:**1b**-FA-NPs were further confirmed by IR spectroscopy. The C=O stretching vibration of **1b** appeared at 1646 $cm^{-1}$ (Figure S12, Supporting Information), and was the strongest absorption in the IR spectrum. After coordination, this peak partly disappeared, and the $\nu_{as}(COO^-)$ mode of a carboxy group appeared at 1615 $cm^{-1}$, and the $\nu_s(COO^-)$ mode at 1383 $cm^{-1}$. The $\Delta\tilde{\nu}$ value $[\tilde{\nu}_{as}(COO^-) - \tilde{\nu}_s(COO^-)]$ was 232 $cm^{-1}$. The $\Delta\tilde{\nu}$ value of Tb:**1b** was higher than that of sodium/**1b**, that is **1b** bonds to $Tb^{III}$ ions through a monodentate carboxy oxygen atom.[13] For Tb:**1b**-FA, both asymmetric ($\nu_{as}$) and symmetric ($\nu_s$) carboxy stretching vibrations were redshifted relative to those of Tb:**1b** (Figure S13, Supporting Information), and the difference $\Delta\tilde{\nu}$ between $\tilde{\nu}_{as}$ and $\tilde{\nu}_s$ was 212 $cm^{-1}$. The absorption of the phenolic hydroxy group appeared at 1458 $cm^{-1}$ in the IR spectrum of Tb:**1b**-FA. The above characteristics were also found for the Tb:4-aminosalicylic acid complex (Figure S14, Supporting Information). This indicates that folate-(salicylic acidyl)-amine coordinates to $Tb^{3+}$ through carboxy and phenolic hydroxy oxygen atoms. For Tb:**1b**-NPs and Tb:**1b**-FA-NPs, peaks at 679, 689, and 601 $cm^{-1}$ are typical Fe–O absorption bands.[14]

The excited-state lifetime of Tb:**1b**-NPs of 1.15 ms is almost identical to that of its complex (1.25 ms),[15] which is long enough for complete decay of the various nonspecific fluorescence and elimination of the background emission from a biological matrix. The quantum yield of Tb:**1b**-NPs is 0.096 in aqueous media.

To evaluate possible cytotoxic effect of Tb:**1b**-NPs, an MTT assay [MTT: 3-(4,5-dimethylthiazol-2-yl)-2,5-diphenyl-

  

tetrazolium bromide] with HeLa cells was used to determine the effect of Tb:**1b**-NPs on cell proliferation after 24 and 48 h (Figure 1A and Figure S15, Supporting Information). No

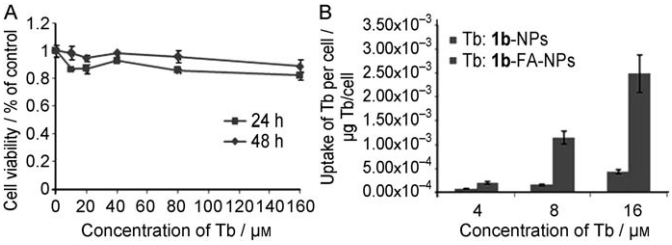


***Figure 1.*** A) Cytotoxic activity of Tb:**1b**-NPs against HeLa cancer cell lines. B) Cell uptake of Tb:**1b**-NPs (left-hand bars) and Tb:**1b**-FA-NPs (right-hand bars) against HeLa cancer cell lines.

significant differences in cell proliferation were observed in the absence or presence of 10–160 μM Tb:**1b**-NPs. Thus, Tb:**1b**-NPs can be considered to have low cytotoxicity. Furthermore, crystal violet staining experiments (Figure S16, Supporting Information) also indicated that Tb:**1b**-NPs has low cytotoxicity in the range of 100–2000 μM.

HeLa cells were incubated with different concentrations of Tb:**1b**-NPs or Tb:**1b**-FA-NPs for 4 h at 37 °C; then they were washed with cold PBS to remove excess nanoparticles. As shown in Figure 1B, uptake of Tb:**1b**-FA-NPs increased with increasing concentration of Tb:**1b**-FA-NPs in the incubating system. Furthermore, association of Tb:**1b**-FA-NPs with HeLa cells was significantly higher than that of Tb:**1b**-NPs. Similar uptake enhancement is also observed for Tb:**1b**-FA-NPs with HeLa cells over Tb:**1b**-FA-NPs with MCF-7 cells (Figure S17, Supporting Information). Therefore, we speculated that Tb:**1b**-FA-NPs were taken up by HeLa cells via the folate receptor.

To evaluate the targeting capability of the luminescent labels of Tb:**1b**-FA-NPs, HeLa (FR-positive) and MCF-7 (FR-negative) cells were incubated in PBS containing 25 g mL$^{-1}$ of Tb:**1b**-FA-NPs at 37 °C for 4 h. For comparison, HeLa cells were also incubated in the presence of Tb:**1b**-NPs (25 g mL$^{-1}$). After washing the cells with PBS to remove excess nanoparticles, they were imaged with a confocal fluorescence microscope. As shown in Figure 2B and Figure S18 (Supporting Information), HeLa cells treated with Tb:**1b**-FA-NPs displayed strong green fluorescence, which

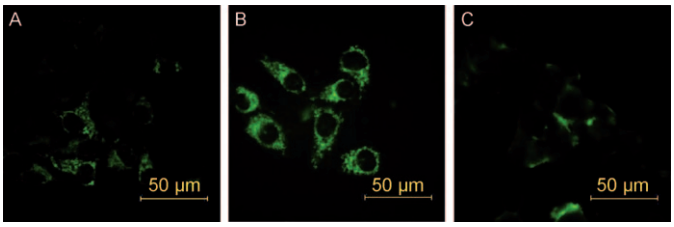


***Figure 2.*** Fluorescence images of HeLa cells after incubation with A) Tb:**1b**-NPs for 5 h and B) Tb:**1b**-FA-NPs for 5 h. C) Fluorescence image of MCF-7 cells after incubation with Tb:**1b**-FA-NPs for 5 h. Emission at (526 ± 19) nm and excitation at (360 ± 40) nm.

can be attributed to the strong specific interaction between FA on Tb:**1b**-FA-NPs and FR on the HeLa cells. In contrast, both MCF-7 cells incubated with Tb:**1b**-FA-NPs (Figure 2C and Figure S19, Supporting Information) and HeLa cells incubated with Tb:**1b**-NPs (Figure 2A and Figure S18, Supporting Information) display weak luminescence, suggesting weak nonspecific binding with the nanoparticles. These results establish that Tb:**1b**-FA-NPs could be used for targeting and imaging HeLa cells with overexpressed FR.

To confirm the magnetic properties of Tb:**1b**-FA-NPs after entering cells, their effect on the relaxation time $T_2$ of free water within the HeLa cells was further tested with magnetic resonance imaging (MRI). Figure 3 shows MRI images obtained from HeLa cells treated with Tb:**1b**-FA-NPs at different concentrations. The images from the cells

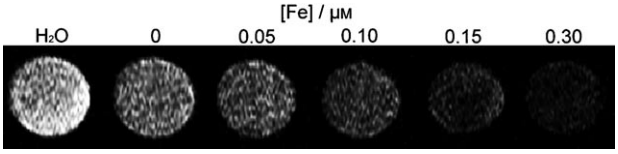


***Figure 3.*** $T_2$-weighted MRI images of HeLa cells containing Tb:**1b**-FA-NPs.

containing Tb:**1b**-FA-NPs become darker with increasing iron concentration, that is, the nanoparticles in the cells do provide contrast enhancement in MRI.

In summary, we have developed a simple method, involving a three-step reaction pathway, to covalently attach luminescent lanthanide complexes to the surface of $Fe_3O_4$ magnetic nanoparticles. The resulting $Fe_3O_4$ NPs show a strong fluorescence and have a long lifetime in DI water. Furthermore, we have shown that this approach using folic acid conjugated Tb:**1b**-FA-NPs enables targeted fluorescent imaging of FR-overexpressing HeLa cell lines in vitro. Due to its superparamagnetic property, low cytotoxicity, and high uptake, Tb:**1b**-FA-NPs could be used as an agent for both fluorescence cell imaging and magnetic resonance imaging.

## *Experimental Section*

Iron(III) acetylacetonate, dibenzyl ether, oleic acid, oleylamine, polyethylene glycol, and 7-amino-4-methyl-2(1*H*)-quinolinone were purchased from Sigma-Aldrich. Folic acid, dicyclohexylcarbodiimide (DCC), 4-aminosalicylic acid, and 3,4-dihydroxybenzaldehyde were obtained from Aladdin in China. All chemicals were used without further purification. 1,ω-Diaminopolyoxyethylene 4000 and diethylenetriaminepentaacetic anhydride (DTPAA) were synthesized according to published methods.[16,17] Cytotoxicity assay and uptake experiments were conducted according to the literature.[18]

HeLa and MCF-7 cell lines were purchased from the Biology Preservation Center in Shanghai Institute of Materia Medica and cultured with Dulbecco's modified Eagle's medium (DMEM, Gibco) supplemented with 10% FBS (Gibco), 2 mM L-glutamine, 100 units mL$^{-1}$ penicillin, and 100 mg mL$^{-1}$ streptomycin and incubated at 37 °C in a humidified atmosphere of 5% $CO_2$ and 95% air.

  

$^1$H NMR spectra were acquired with a Varian 200 MHz NMR spectrometer. TEM images were taken on a Philips EM 420 (120 kV) and fluorescence images on a Zeiss Leica inverted epifluorescence/reflectance laser scanning confocal microscope. The UV/vis spectra were recorded on a Varian Cary 100 Conc spectrophotometer and the fluorescence spectra on a Hitachi RF-4500 spectrofluorophotometer. IR spectra (4000–400 $cm^{-1}$) were determined with KBr disks on a Therrno Mattson FTIR spectrometer.

Details on the syntheses of the compounds and the experiments on their anticancer activity can be found in the Supporting Information.

Received: October 3, 2010
Revised: January 13, 2011
Published online: March 1, 2011

**Keywords:** fluorescence · lanthanides · magnetic properties · MRI contrast agents · nanoparticles

[1] J.-L. Bridot, A.-C. Faure, S. Laurent, C. Rivière, C. Billotey, B. Hiba, M. Janier, V. Josserand, J.-L. Coll, L. Vander Elst, R. Muller, S. Roux, P. Perriat, O. Tillement, *J. Am. Chem. Soc.* **2007**, *129*, 5076 – 5084.

[2] a) A. H. Latham, M. E. Williams, *Acc. Chem. Res.* **2008**, *41*, 411; b) C. Xu, S. Sun, *Polym. Int.* **2007**, *56*, 821; c) Y.-W. Jun, J.-W. Seo, J. Cheon, *Acc. Chem. Res.* **2008**, *41*, 179.

[3] a) J. Rao, A. Dragulescu-Andrasi, H. Yao, *Curr. Opin. Biotechnol.* **2007**, *18*, 17; b) Z. Cheng, J. Levi, Z. M. Xiong, O. Gheysens, S. Keren, X. Y. Chen, S. S. Gambhir, *Bioconjugate Chem.* **2006**, *17*, 662 – 669; c) B. A. Smith, W. J. Akers, W. M. Leevy, A. J. Lampkins, S. Z. Xiao, W. Wolter, M. A. Suckow, S. Achilefu, B. D. Smith, *J. Am. Chem. Soc.* **2010**, *132*, 67 – 69.

[4] a) J. J. Yu, D. Parker, R. Pal, R. A. Poole, M. J. Cann, *J. Am. Chem. Soc.* **2006**, *128*, 2294; b) J. P. Leonard, P. Jensen, T. McCabe, J. E. O′Brien, R. D. Peacock, P. E. Kruger, T. Gunnlaugsson, *J. Am. Chem. Soc.* **2007**, *129*, 10986.

[5] L. F. Hu, R. Z. Ma, T. C. Ozawa, T. Sasaki, *Angew Chem.* **2009**, *121*, 3904 – 3907; *Angew Chem. Int. Ed.* **2009**, *48*, 3846 – 9.

[6] a) P. H. Lin, S. H. Wang, S. L. Chang, *Spectrosc. Spectral Anal.* **2007**, *27*, 123; b) Z. Zhang, W. L. Pan, *Fine Spec. Chem.* **2007**, *15*, 15.

[7] J. Xie, C. J. Xu, N. Kohler, Y. L. Hou, S. H. Sun, *Adv. Mater.* **2007**, *19*, 3163 – 3156.

[8] C. J. Xu, B. D. Wang, S. H. Sun, *J. Am. Chem. Soc.* **2009**, *131*, 4216 – 4217.

[9] C. J. Xu, J. Xie, N. Kohler, E. G. Walsh, Y. E. Chin, S. H. Sun, *Chem. Asian J.* **2008**, *3*, 548 – 552.

[10] J. Xie, C. J. Xu, Z. C. Xu, Y. L. Hou, K. L. Young, S. X. Wang, N. Pourmand, S. H. Sun, *Chem. Mater.* **2006**, *18*, 5401 – 5403.

[11] a) P. R. Selvin, J. Jancarik, M. Li, L. W. Hung, *Inorg. Chem.* **1996**, *35*, 700 – 705; b) M. S. Tremblay, M. Halim, D. Sames, *J. Am. Chem. Soc.* **2007**, *129*, 7570 – 7577.

[12] F. S. Richardson, *Chem. Rev.* **1982**, *82*, 541.

[13] K. Nakamoto, *Infrared and Raman Spectra of Inorganic and Coordination Compounds*, 4th ed., Wiley, New York, **1986**.

[14] M. Ma, Y. Zhang, W. Yu, H. Y. Shen, H. Q. Zhang, N. Gu, *Colloids Surf. A* **2003**, *212*, 219 – 226.

[15] M. Li, P. R. Selvin, *Bioconjugate Chem.* **1997**, *8*, 127 – 132.

[16] O. A. Aronov, T. Horowitz, A. Gabizon, D. Gibson, *Bioconjugate Chem.* **2003**, *14*, 563 – 574.

[17] Y. M. Wang, T. H. Cheng, *J. Chem. Soc. Dalton Trans.* **1997**, *6*, 833 – 837.

[18] B. D. Wang, C. J. Xu, J. Xie, Z. Y. Yang, S. H. Sun, *J. Am. Chem. Soc.* **2008**, *130*, 14436 – 14437.

  